

N89 - 15185

53-24
182077
418

FRACTURE ANALYSIS OF LOCAL DELAMINATIONS IN LAMINATED COMPOSITES

P. Sriram and E. A. Armanios
School of Aerospace Engineering
Georgia Institute of Technology
Atlanta, Georgia 30332

Abstract

Delamination is a predominant failure mode in continuous fiber reinforced laminated composite structures. One type of delamination is the transverse crack tip delamination which originates at the tip of transverse matrix cracks. An analytical model based on the sublaminar approach and fracture mechanics is developed in this paper to study the growth of such delaminations. Plane strain conditions are assumed and estimates are provided for the total strain energy release rate as well as the mode I and mode II contributions. The energy release rate estimates are used to predict critical delamination growth strains and stresses by assuming a critical energy release rate. These predictions are compared with experimental data on T300/934 Graphite Epoxy $[\pm 25/90_n]_s$ laminates in the range $n=5$ to 8. A good agreement is demonstrated for the range of n where the experimental observations indicate transverse crack tip delamination to be the predominant failure mode.

Introduction

Fiber reinforced composites are now being used in a wide variety of engineering structures. The concept of directional strength and stiffness has been, for the most part, understood sufficiently to enable efficient load bearing designs. One of the current major issues in composite structures is the understanding and prediction of damage modes and failure mechanisms. A thorough knowledge of the failure mechanisms is bound to lead to the design of efficient and durable structures. Failures in these materials often initiate in the form of matrix cracks or delaminations.

Matrix cracks refer to intralaminar failures whereas delaminations refer to interlaminar failures.

Matrix cracks usually occur within laminates where the fibers run at an angle to the primary load direction. Hence, such matrix cracks are also called transverse cracks. Based on the location and direction of growth, two distinct types of delamination can be discerned. These two types are called edge delamination and local or transverse crack tip delamination. Edge delaminations initiate at the load free edges of the structure whereas local delaminations start from a transverse matrix crack. In many cases, both types occur concurrently with varying levels of interaction. It has been observed in simple tension tests of uniform rectangular cross section specimen (Edge Delamination test) that delaminations initiate along the load free edges and propagate normal to the load direction. Transverse matrix cracks running parallel to the fibers have also been observed in off axis plies such as 90° plies. Such transverse cracks terminate where the ply orientation changes. Delaminations can originate at the interface where transverse cracks terminate. These delaminations, called transverse crack delaminations or local delaminations, grow normal to the transverse crack from which they originate. In the case of 90° plies, the growth direction is parallel to the load.

The growth process of edge delaminations and local delaminations is often modelled using a fracture mechanics approach leading to the calculation of a strain energy release rate. This is because the strain energy release rate can correlate delamination behavior from different loading conditions and can account for geometric dependencies. The strain energy release rate associated with a particular growth configuration is a measure of the driving force behind that failure mode. In combination with

appropriate failure criteria, the strain energy release rate provides a means of predicting the failure loads of the structure.

Several methods are available in the literature for analyzing edge delaminations. These include finite element modelling¹⁻³, complex variable stress potential approach⁴, simple classical laminate theory based technique⁵ and higher order laminate theory including shear deformations⁶. Finite element models provide accurate solutions but involve intensive computational effort. Classical laminate theory (CLT) based techniques provide simple closed form solutions and are thus well suited for preliminary design evaluation. Classical laminate theory based techniques provide only the total energy release rate, and thus in a mixed mode situation, there is insufficient information to completely assess the delamination growth tendency. A higher order laminate theory including shear deformations has the ability to provide the individual contributions of the three fracture modes while retaining the simplicity of a closed form solution. A shear deformation model is available for edge delamination and has been shown to agree well with finite element predictions⁶.

Crossman and Wang⁷ have tested T300/934 Graphite epoxy $[\pm 25/90_n]_s$ specimens in simple tension and reported a range of behavior including transverse cracking, edge delamination and local delamination. O'Brien⁸ has presented classical laminate theory solutions for these specimen, demonstrating reasonable agreement in the case of edge delamination but with some discrepancies in the local delamination predictions. An empirical finite element based combined edge and local delamination formulation has also been proposed⁹. Its predictions, however, do not fully explain the dependency of the critical strain on the number of 90° plies.

In this paper, a shear deformation model is developed for the analysis of local delaminations originating from transverse cracks in 90° plies

located in and around the specimen midplane. Plane strain conditions are assumed and thickness strain is neglected. Delaminations are assumed to grow from both ends of the transverse crack tip. The transverse crack is treated as a free boundary and the delamination is considered to be the crack whose growth behavior is to be modelled. The sublamine approach^{10,11} is used to model different regions of the specimen. The resulting boundary value problem is solved to obtain the interlaminar stresses, total strain energy release rate and energy release rate components. Critical local delamination growth loads are predicted for the $[\pm 25/90_n]_s$ specimen.

Analytical Model

The formulation is based on the sublamine approach detailed in ref. 10. A longitudinal section illustrating the geometry of a generic configuration is shown in fig. 1. The central region is assumed to be made of 90° plies with an isolated transverse crack in the middle. Delaminations are assumed to grow from both ends of the transverse crack, and towards both ends as shown. From symmetry considerations, only one quarter of the configuration is modelled. The modelled portion is divided into four sublaminae as shown in fig. 2. The top surface (sublaminae 1 and 4) is stress free. In order to simplify the analysis, plane strain conditions are assumed and the thickness strain (ϵ_z) is set to zero. The consequence of this combined with the fact that the w displacement is zero along the center line is that w is zero in sublaminae 1, 2 and 3. Further, this approximation does not allow for the enforcement of boundary conditions on the shear stress resultants, leading to incorrect estimates of the interlaminar normal stresses. The interlaminar shear stresses, however, are not affected by this assumption^{6,10}. The assumptions lead to considerable simplifications in the analysis. In spite of the simplifications, reliable

energy release rate components can be estimated based on the interlaminar shear stress distributions^{6,10}.

A generic sublaminar is shown in fig. 3 along with the notations and sign conventions. The peel and interlaminar shear stresses are denoted by P and T respectively with t and b subscripts for the top and bottom surface respectively. The axial stress resultant, shear stress resultant and bending moment resultant are denoted by N , Q and M respectively. A summary of the governing equations is presented here for convenience. These are derived for a generic sublaminar using the principle of virtual work in Reference 12.

The x and z displacements within the sublaminar are assumed to be of the form

$$u(x,z)=U(x)+z\beta(z) \quad (1)$$

$$w(x,z)=W(x). \quad (2)$$

Here U represents the axial midplane stretching and W is the transverse displacement. The shear deformation is recognized through the rotation β . The origin of the coordinate axes for the sublaminars is taken at the delamination tip as shown in fig. 4. The equilibrium equations take the form

$$N_{,x}+T_t-T_b=0 \quad (3)$$

$$Q_{,x}+P_t-P_b=0 \quad (4)$$

$$M_{,x}-Q+(h/2)(T_t+T_b)=0. \quad (5)$$

where h is the thickness of the sublaminar. The constitutive relations in terms of the force and moment resultants are

$$N=A_{11}U_{,x}+B_{11}\beta_{,x} \quad (6)$$

$$Q=A_{55}(\beta+W_{,x}) \quad (7)$$

$$M=B_{11}U_{,x}+D_{11}\beta_{,x} \quad (8)$$

where the A_{ij} , B_{ij} and D_{ij} are the classical laminate theory axial, coupling and bending stiffnesses. The boundary variables to be prescribed at the sublamine edges are

N or U

M or β

Q or W.

Additionally, at the interfaces between sublaminae, reciprocal traction and displacement matching boundary conditions have to be specified.

Solution Procedure

A detailed solution is provided in the Appendix. A brief summary is provided here for convenience. The variables in sublaminae 1 and 2 are coupled by their reciprocal interlaminar stresses denoted T_1 and P_1 and by displacement continuity at their common interface. Assuming exponential solutions for the axial force and bending moment resultants ($N_1 = Ae^{sx}$, $M_1 = Be^{sx}$ etc.) leads to an eigen value problem involving the parameter s . The eigen values turn out to be 0 and two nonzero values (say s_1 and s_2) occurring in positive and negative pairs. Since the resultants maintain finite values as x tends to large negative values (left end of sublaminae 1 and 2), the negative roots are dropped out of the solution.

The following boundary conditions from the ends of the modelled region are enforced.

$$N_2(0) = 0 \quad (9)$$

$$Q_4(a) = 0 \quad (10)$$

$$\beta_4(a) = 0 \quad (11)$$

$$N_1 + N_2 = \text{Applied Load} \quad (12)$$

Further, the following displacement matching conditions are applied.

$$u_1(x, -.5h_1) = u_2(x, .5h_2) \quad (13)$$

$$U_1(0) = U_4(0) \quad (14)$$

$$U_2(0)=U_3(0) \quad (15)$$

$$\beta_1(0)=\beta_4(0) \quad (16)$$

It should be noted that a β_2 and β_3 matching condition cannot be applied at this level of modeling since it would amount to specifying both W and $Q^{6,12}$. Consequently, there is a displacement discontinuity at the delamination tip. The effect of this will be discussed subsequently. To eliminate rigid body displacements, U_1 is set to zero at the left end. The following solutions can then be obtained for the resultants in sublaminates 1 and 2.

$$N_1=a_1e^{s_1x}+a_2e^{s_2x}+\epsilon A_{11}(1) \quad (17)$$

$$N_2=-a_1e^{s_1x}-a_2e^{s_2x}+\epsilon A_{11}(2) \quad (18)$$

$$M_1=a_1k_1e^{s_1x}+a_2k_2e^{s_2x} \quad (19)$$

$$M_2=a_1k_3e^{s_1x}+a_2k_4e^{s_2x} \quad (20)$$

The interlaminar shear and peel stresses between sublaminates 1 and 2 can be obtained as

$$T_1=a_1s_1e^{s_1x}+a_2s_2e^{s_2x} \quad (21)$$

$$P_1=(k_1+.5h_1)(a_1s_1^2e^{s_1x})+(k_2+.5h_1)(a_2s_2^2e^{s_2x}) \quad (22)$$

In the above solutions, the k parameters are dependent on the eigen values and the stiffness of sublaminates 1 and 2, the a parameters depend on the k parameters and the initial crack length a , and ϵ is defined as

$$\epsilon=\sigma(h_1+h_2)/(A_{11}(1)+A_{11}(2)) \quad (23)$$

where σ is the applied uniform axial stress. Complete expressions for the eigen values and the a and k parameters can be found in the Appendix.

Proceeding on to sublaminates 3 and 4, the following solutions can be written.

$$N_3=0 \quad (24)$$

$$M_3=\phi_1 \sinh \omega_3 x + \phi_2 \cosh \omega_3 x \quad (25)$$

where

$$\phi_2=a_1k_3+a_2k_4, \quad (26)$$

$$\phi_1 = -\phi_2 \coth \omega_3 a \quad (27)$$

and
$$\omega_3 = (A_{55}(2)/D_{11}(2))^{0.5} \quad (28)$$

$$N_4 = \varepsilon (A_{11}(1) + A_{11}(2)) \quad (29)$$

$$M_4 = a_1 k_1 + a_2 k_2 \quad (30)$$

The corresponding displacement solutions are provided in the Appendix.

The compliance of the specimen can be evaluated as

$$C = 2U_4(a)/P \quad (31)$$

where $P/2$ is the load applied to the modelled section. The total energy release rate for the modelled section i.e. the total energy release rate G_T per crack is then given by

$$G_T = P^2/2w (dC/da) \quad (32)$$

where w is the specimen width. Use of the previously described solutions leads to the following expression.

$$G_T = \frac{P^2}{2w^2} \left(\frac{1}{A_{11(1)}} - \frac{1}{A_{11(1)} + A_{11(2)}} + I_1 - I_2 \right) \quad (33)$$

where the quantities I_1 and I_2 contain exponential terms dependent on the initial delamination length. Using the virtual crack closure technique, from the relative displacements in the cracked portion and the interlaminar stresses ahead of the crack tip, the mode I and mode II energy release rate contributions can be obtained. The mode III energy release rate is zero from the assumption of plane strain. The mode II energy release rate is given by

$$G_{II} = \lim_{\delta \rightarrow 0} \frac{1}{2\delta} \int_0^\delta T_{II}(x - \delta) \Delta u(x) dx \quad (34)$$

where δ is the virtual crack step size. The result of the limiting process is zero if there is no singularity in the stress field¹⁰. So, the limit is usually taken as the crack step size δ tends to a small value, say Δ , based on the decay length or the length required to capture the essential features of the stress and displacement fields near the crack tip. The decay

length is dependent on the eigen values s_1 and s_2 . In this study, the value of Δ has been set to

$$\Delta_0 = .25(1/s_1 + 1/s_2) \quad (35)$$

since it reasonably fulfills the criterion given above. In a similar fashion, the mode I energy release rate can be obtained based on the normal stress (P) and the w displacements near the crack front. The normal (peel) stress estimate is inaccurate due to the absence of thickness strain. Hence, an alternate approach was used to estimate G_I , the mode I energy release rate. The total energy release rate for this problem is made up entirely of G_I and G_{II} ($G_{III}=0$). From an estimate of G_T and G_{II} , an estimate for G_I can be obtained simply as

$$G_I = G_T - G_{II} \quad (36)$$

The critical load for a given specimen can then be evaluated based on an appropriate fracture law. This is illustrated in the following section.

Results and Discussion

The solutions derived in the previous section have been used to model the behavior of $[\pm 25/90_n]_S$ T300/934 Graphite Epoxy specimen for n values of .5, 1, 2, 3, 4, 6, and 8. These correspond to the specimen tested by Crossman and Wang⁷. The specimen width and length were fixed at .0381 m and .015m respectively, as in the tests. The solutions were generated using a simple computer program based on the closed form expressions for the interlaminar stress and energy release rates. The applied load was set to 100 MPa, of the same order as in the tests.

An example of the total energy release rate variation with the crack length is presented in fig. 5. The asymptotic value of G_T is denoted by G_{T0} in the figure. It can be observed that after a certain crack length, the G_T is independent of the crack length. On the basis of curves like the one shown in fig. 5, the crack length was fixed at 10 ply thicknesses for

the remainder of the study. The dependence of the mode II contribution of the energy release rate on initial crack length (a) is depicted in fig. 6. Typical interlaminar shear and normal stress profiles are presented in figs. 7 and 8 respectively. The corresponding energy release rates have also been calculated and are presented in Table 1 and fig. 9.

In order to evaluate the critical loads, an appropriate mixed mode fracture law has to be applied, based on the calculated energy release components. Since the calculated mode split shows only a small variation with n , the simple Griffith criterion $G_T = G_{TC}$ has been used to scale the stresses to obtain the critical delamination growth stress (σ_c) and strain (ϵ_c) values. The critical energy release rate G_{TC} was chosen as 415 J/m^2 to obtain the critical stresses and strains listed in Table 1. This value of G_{TC} is larger than G_{IC} to account for the presence of mode II and the fact that G_{IIc} is about four times G_{IC} for the material system under consideration. The critical strains are plotted against n , the number of 90° plies in fig. 10. The experimental results of ref. 7 and the predictions of refs. 8 and 9 are also presented in the figure for comparison. The predictions of the model developed in this paper are represented by the solid line while the experimental results are shown as filled squares. The classical laminate theory and finite element critical strain predictions of refs. 8 and 9 are represented by triangles with a connecting line and a dotted line respectively.

In the experiments, the local delamination phenomenon was observed as the predominant failure mode only for the $n=4,6$ and 8 specimens. The shear deformation model presented in this paper provides good agreement with the experimental data in this range. For $n < 4$, edge delamination either in the mid plane or in the 25/90 interface was observed in the tests. Hence, the predictions of the local delamination models in this region are not of

consequence as long as they do not predict critical loads lower than those predicted by edge delamination models. Thus, it can be seen that the shear deformation model predicts the observed behavior with reasonable accuracy and can be used in conjunction with an appropriate edge delamination model to predict critical loads accurately for the complete range of n values. The edge delamination model presented in References 6 and 12 can be used for this purpose. However, a separate model is required to account for the mid-plane (Mode I) edge delamination behavior.

Conclusions

A shear deformation model has been developed to analyze local delaminations growing from transverse cracks in 90° plies located around the mid plane of symmetric laminates. The predictions of the model agree reasonably with experimental data from $[\pm 25/90_n]_S$ T300/934 Graphite Epoxy laminates. The predicted behavior is such that, in combination with an edge delamination model, the critical loads can be predicted accurately in the range of n from .5 to 8.

Acknowledgements

The authors gratefully acknowledge the financial support provided by NASA under grant NAG-1-637 for performing the research reported in this paper. The authors also wish to thank Mr. A. Badir for help in verifying the analytical model.

References

- [1] Wilkins, D.J., Eisemann, J.R., Camin, R.A., Margolis, W.S. and Benson, R.A., "Characterizing Delamination Growth in Graphite-Epoxy," in Damage in Composite Materials, ASTM STP 775, K.L. Reifsnider, Ed., pp. 168-183 (1982).

- [2] O'Brien, T.K., "Mixed-Mode Strain Energy Release Rate Effects on Edge Delamination of Composites," in Effects of Defects in Composite Materials, ASTM STP 836, pp. 125-142 (1984).
- [3] Wang, S.S. and Choi, I., "The Mechanics of Delamination in Fiber Reinforced Composite Materials. Part II - Delamination Behavior and Fracture Mechanics Parameters," NASA CR-172270 (1983).
- [4] Wang, S.S., "Edge Delamination in Angle Ply Composite Laminates," Proceedings of the 22nd AIAA/ASME/ASCE/AHS Structures, Structural Dynamics and Materials (SDM) Conference, Atlanta, Georgia, 6-8 April, 1981, pp. 473-484.
- [5] O'Brien, T.K., "Characterization of Delamination Onset and Growth in a Composite Laminate," in Damage in Composite Materials, ASTM STP 775, K.L. Reifsnider, Ed., pp. 140-167 (1982).
- [6] Armanios, E.A., and Rehfield, L.W., "Interlaminar Analysis of Laminated Composites using a Sublaminar Approach," Proceedings of the 27th AIAA/ASME/ASCE/AHS Structures, Structural Dynamics and Materials (SDM) Conference, San Antonio, Texas, 19-21 May, 1986, Part 1, pp. 442-452. AIAA Paper 86-0969CP.
- [7] Crossman, F.W., and Wang, A.S.D., "The Dependence of Transverse Cracking and Delamination on Ply Thickness in Graphite/Epoxy Laminates," in Damage in Composite Materials, ASTM STP 775, K.L. Reifsnider, Ed., pp. 118-139 (1982).
- [8] O'Brien, T.K., "Analysis of Local Delaminations and Their Influence on Composite Laminate Behavior," in Delamination and Debonding of Materials, ASTM STP 876, Johnson, W.S., Ed., pp. 282-297 (1985).
- [9] Law, G.E., "A Mixed Mode Fracture Analysis of $(\pm 25/90_n)_s$ Graphite/Epoxy Composite Laminates," in Effects of Defects in Composite Materials, ASTM STP 836, pp. 143-160 (1984).

- [10] Armanios, E.A., "New Methods of Sublamine Analysis for Composite Structures and Applications to Fracture Processes," Ph.D. Thesis, Georgia Institute of Technology (1984).
- [11] Armanios, E.A., Rehfield, L.W., and Reddy, A.D., "Design Analysis and Testing for Mixed-Mode and Mode II Interlaminar Fracture of Composites," in Composite Materials: Testing and Design (Seventh Conference), ASTM STP 893, J.M. Whitney, Ed., pp. 232-255 (1986).
- [12] Armanios, E.A., and Rehfield, L.W., "Sublamine Analysis of Interlaminar Fracture in Composites: Part I - Analytical Model", submitted for publication in the Journal of Composites Technology and Research (July, 1988).

Appendix A

Sublamine Analysis for Local Delaminations

Interlaminar Stresses and Energy Release Rates

A generic sublamine is shown in figure 3 along with the notations and sign conventions. The interlaminar normal (peel) and shear stresses are denoted by P and T respectively with the t and b subscripts for the top and bottom surfaces respectively. The axial force resultant, shear force resultant and bending moment resultant are denoted by N , Q and M respectively. Plane strain conditions are assumed to prevail in the $x-z$ plane and the thickness strain ϵ_{zz} is neglected. These assumptions lead to considerable simplification in the analysis. The displacements in the x and z directions are assumed to be of the form

$$u = U(x) + z\beta(x) \quad (\text{A.1})$$

$$w = W(x) \quad (\text{A.2})$$

Here U represents the axial stretching and W is the transverse (thickness direction) displacement. This formulation recognizes shear deformation through the rotation β . The equilibrium equations take the form

$$N_{,x} + T_t - T_b = 0 \quad (\text{A.3})$$

$$Q_{,x} + P_t - P_b = 0 \quad (\text{A.4})$$

$$M_{,x} - Q + \frac{h}{2}(T_t + T_b) = 0 \quad (\text{A.5})$$

where h is the thickness of the sublaminate. The constitutive equations in terms of the force and moment resultants are

$$N = A_{11}U_{,x} + B_{11}\beta_{,x} \quad (\text{A.6})$$

$$Q = A_{55}(\beta + W_{,x}) \quad (\text{A.7})$$

$$M = B_{11}U_{,x} + D_{11}\beta_{,x} \quad (\text{A.8})$$

where A, B and D are the classical laminate theory axial, coupling and bending stiffnesses defined in the customary manner as

$$\begin{aligned} A_{11} &= \int_{-\frac{h}{2}}^{\frac{h}{2}} C_{11} dz \\ B_{11} &= \int_{-\frac{h}{2}}^{\frac{h}{2}} C_{11} z dz \\ D_{11} &= \int_{-\frac{h}{2}}^{\frac{h}{2}} C_{11} z^2 dz \\ A_{55} &= \int_{-\frac{h}{2}}^{\frac{h}{2}} C_{55} dz \end{aligned}$$

Here, the C s are the material moduli. For the case of plane strain in the $x - z$ plane, the C s are defined as follows.

$$\begin{Bmatrix} \sigma_{xx} \\ \sigma_{zz} \\ \tau_{xz} \end{Bmatrix} = \begin{bmatrix} C_{11} & C_{13} & 0 \\ C_{13} & C_{22} & 0 \\ 0 & 0 & C_{55} \end{bmatrix} \begin{Bmatrix} \epsilon_{xx} \\ \epsilon_{zz} \\ \gamma_{xz} \end{Bmatrix} \quad (\text{A.9})$$

The boundary quantities to be prescribed at the sublaminate edges are

$$N \quad \text{or} \quad U$$

$$M \quad \text{or} \quad \beta$$

$$Q \quad \text{or} \quad W$$

Further, at the interfaces between sublaminates, appropriate reciprocal traction and displacement matching boundary conditions have to be used.

The four sublaminates along with the loads acting on each are shown in figure 4. Setting P_1 and T_1 as shown automatically satisfies the traction matching boundary condition at the 1-2 interface. From symmetry, we get $w = 0$ and zero shear stress along the bottom faces of sublaminates 2 and 3. This leads to $w = 0$ in sublaminates 1, 2 and 3. Thus, W has been prescribed in these sublaminates and the vertical shear force resultant Q cannot be prescribed at both ends of the sublaminates. Consequently, the calculated peel stress distribution will not be correct. In addition, at the 2-3 interface, the β s cannot be matched, since in these sublaminates, specifying β is equivalent to specifying Q (through eq. A.7). In spite of these simplifications, reliable energy release rate components can be estimated based on the interlaminar shear stress distributions. The mode I contribution can then be evaluated using the total energy release rate, which is not affected significantly by these simplifications.

For the $(\pm 25/90_n)_s$ laminates under consideration, B_{11} is zero in all the four sublaminates. For sublaminates 1 and 2, the equilibrium equations and constitutive relationships can be written as

$$N_{1,x} - T_1 = 0 \quad (\text{A.10})$$

$$N_{2,x} + T_1 = 0 \quad (\text{A.11})$$

$$Q_{1,x} - P_1 = 0 \quad (\text{A.12})$$

$$Q_{2,x} + P_1 - P_2 = 0 \quad (\text{A.13})$$

$$M_{1,x} + \frac{h_1}{2} T_1 - Q_1 = 0 \quad (\text{A.14})$$

$$M_{2,x} + \frac{h_2}{2} T_1 - Q_2 = 0 \quad (\text{A.15})$$

$$N_1 = A_{11(1)} U_{1,x} \quad (\text{A.16})$$

$$N_2 = A_{11(2)}U_{2,x} \quad (\text{A.17})$$

$$Q_1 = A_{55(1)}\beta_1 \quad (\text{A.18})$$

$$Q_2 = A_{55(2)}\beta_2 \quad (\text{A.19})$$

$$M_1 = D_{11(1)}\beta_{1,x} \quad (\text{A.20})$$

$$M_2 = D_{11(2)}\beta_{2,x} \quad (\text{A.21})$$

The subscripts in brackets refer to the sublaminae to which the stiffness coefficients correspond. Equations A.14, A.15 and A.12 can be rewritten in a modified form as

$$M_{1,x} + \frac{h_1}{2}N_{1,x} = A_{55(1)}\beta_1 \quad (\text{A.22})$$

$$M_{2,x} - \frac{h_2}{2}N_{2,x} = A_{55(2)}\beta_2 \quad (\text{A.23})$$

$$\begin{aligned} P_1 &= Q_{1,x} \\ &= M_{1,xx} + \frac{h_1}{2}T_{1,x} \end{aligned} \quad (\text{A.24})$$

Matching the u displacement along the 1-2 interface implies

$$\begin{aligned} u_1\left(-\frac{h_1}{2}, x\right) &= u_2\left(\frac{h_2}{2}, x\right) \\ \text{or } U_1 - \frac{h_1}{2}\beta_1 &= U_2 + \frac{h_2}{2}\beta_2 \end{aligned} \quad (\text{A.25})$$

Combining the equations to eliminate the displacement and interlaminar stress terms leads to the following homogeneous coupled system of ordinary differential equations.

$$N_{1,x} + N_{2,x} = 0 \quad (\text{A.26})$$

$$M_{1,xx} + \frac{h_1}{2}N_{1,xx} - \frac{A_{55(1)}}{D_{11(1)}}M_1 = 0 \quad (\text{A.27})$$

$$M_{2,xx} - \frac{h_2}{2}N_{2,xx} - \frac{A_{55(2)}}{D_{11(2)}}M_2 = 0 \quad (\text{A.28})$$

$$\frac{N_1}{A_{11(1)}} - \frac{h_1}{2}\frac{M_1}{D_{11(1)}} - \frac{N_2}{A_{11(2)}} - \frac{h_2}{2}\frac{M_2}{D_{11(2)}} = 0 \quad (\text{A.29})$$

The solution is assumed of the form

$$\begin{Bmatrix} N_1 \\ N_2 \\ M_1 \\ M_2 \end{Bmatrix} = \begin{Bmatrix} A_1 \\ A_2 \\ A_3 \\ A_4 \end{Bmatrix} e^{sx} \quad (\text{A.30})$$

Substitution of this solution into the governing equations results in the following system of algebraic equations.

$$\begin{bmatrix} s & s & 0 & 0 \\ s^2 \frac{h_1}{2} & 0 & s^2 - \frac{A_{55(1)}}{D_{11(1)}} & 0 \\ 0 & -s^2 \frac{h_2}{2} & 0 & s^2 - \frac{A_{55(2)}}{D_{11(2)}} \\ \frac{1}{A_{11(1)}} & -\frac{1}{A_{11(2)}} & -\frac{h_1}{2} \frac{1}{D_{11(1)}} & -\frac{h_2}{2} \frac{1}{D_{11(2)}} \end{bmatrix} \begin{Bmatrix} A_1 \\ A_2 \\ A_3 \\ A_4 \end{Bmatrix} e^{sx} = \begin{Bmatrix} 0 \\ 0 \\ 0 \\ 0 \end{Bmatrix} \quad (\text{A.31})$$

The corresponding eigenvalue problem has to be solved in order to obtain non trivial solutions. The eigenvalues turn out to be the roots of the following characteristic equation.

$$s [B_1 s^4 + B_2 s^2 + B_3] = 0 \quad (\text{A.32})$$

where

$$\begin{aligned} B_1 &= -\frac{1}{A_{11(2)}} - \frac{1}{A_{11(1)}} - \frac{1}{D_{11(2)}} \left(\frac{h_2}{2}\right)^2 - \frac{1}{D_{11(1)}} \left(\frac{h_1}{2}\right)^2 \\ B_2 &= \frac{1}{A_{11(2)}} \frac{A_{55(2)}}{D_{11(2)}} + \frac{1}{A_{11(2)}} \frac{A_{55(1)}}{D_{11(1)}} + \frac{A_{55(1)}}{D_{11(1)}} \frac{1}{D_{11(2)}} \left(\frac{h_2}{2}\right)^2 \\ &\quad + \frac{1}{A_{11(1)}} \frac{A_{55(1)}}{D_{11(1)}} + \frac{1}{A_{11(1)}} \frac{A_{55(2)}}{D_{11(2)}} + \frac{A_{55(2)}}{D_{11(2)}} \frac{1}{D_{11(1)}} \left(\frac{h_1}{2}\right)^2 \\ B_3 &= -\frac{1}{A_{11(2)}} \frac{A_{55(1)}}{D_{11(1)}} \frac{A_{55(2)}}{D_{11(2)}} - \frac{1}{A_{11(1)}} \frac{A_{55(1)}}{D_{11(1)}} \frac{A_{55(2)}}{D_{11(2)}} \end{aligned}$$

For the material system and ply stacking sequence considered, $B_2^2 > 4B_1B_3$. Hence, the roots can be written as

$$s = 0, \pm \sqrt{\frac{-B_2 \pm \sqrt{B_2^2 - 4B_1B_3}}{2B_1}} \quad (\text{A.33})$$

Only the zero and positive roots of eq. A.33 are considered as they give exponentially decaying solutions, leading to finite values for the resultants at the sublaminate ends. Hence, the solution for N_1 can be written as

$$N_1 = a_1 e^{s_1 x} + a_2 e^{s_2 x} + \alpha_1 \quad (\text{A.34})$$

Using this in eq. A.26 yields

$$N_2 = -a_1 e^{s_1 x} - a_2 e^{s_2 x} + \alpha_2 \quad (\text{A.35})$$

Substituting N_1 and N_2 in eqs. A.27 and A.28 provides the solutions for the bending moments as

$$M_1 = a_1 k_1 e^{s_1 x} + a_2 k_2 e^{s_2 x} \quad (\text{A.36})$$

$$M_2 = a_1 k_3 e^{s_1 x} + a_2 k_4 e^{s_2 x} \quad (\text{A.37})$$

The k parameters in the above solutions are defined as follows.

$$k_1 = \frac{\frac{h_1}{2} s_1^2}{\frac{A_{55(1)}}{D_{11(1)}} - s_1^2} \quad (\text{A.38})$$

$$k_2 = \frac{\frac{h_1}{2} s_2^2}{\frac{A_{55(1)}}{D_{11(1)}} - s_2^2} \quad (\text{A.39})$$

$$k_3 = \frac{\frac{h_2}{2} s_1^2}{\frac{A_{55(2)}}{D_{11(2)}} - s_1^2} \quad (\text{A.40})$$

$$k_4 = \frac{\frac{h_2}{2} s_2^2}{\frac{A_{55(2)}}{D_{11(2)}} - s_2^2} \quad (\text{A.41})$$

If P is the applied force and w represents the specimen width,

$$N_1 + N_2 = \frac{P}{2w} \quad (\text{A.42})$$

Using this in conjunction with eq. A.29 allows determination of the constants α_1 and α_2 . The following solutions for the stresses and the resultants can then be obtained.

$$N_1 = a_1 e^{s_1 x} + a_2 e^{s_2 x} + \frac{P}{2w} \frac{A_{11(1)}}{A_{11(1)} + A_{11(2)}} \quad (\text{A.43})$$

$$N_2 = -a_1 e^{s_1 x} - a_2 e^{s_2 x} + \frac{P}{2w} \frac{A_{11(2)}}{A_{11(1)} + A_{11(2)}} \quad (\text{A.44})$$

$$\begin{aligned} T_1 &= N_{1,x} \\ &= a_1 s_1 e^{s_1 x} + a_2 s_2 e^{s_2 x} \end{aligned} \quad (\text{A.45})$$

$$\begin{aligned} P_1 &= M_{1,xx} + \frac{h_1}{2} T_{1,x} \\ &= (k_1 + \frac{h_1}{2}) a_1 s_1^2 e^{s_1 x} + (k_2 + \frac{h_1}{2}) a_2 s_2^2 e^{s_2 x} \end{aligned} \quad (\text{A.46})$$

The constitutive equations are used to write down the displacement solutions. The rigid body displacements of sublaminates 1 and 2 are matched (in order to satisfy the displacement continuity condition) to obtain

$$U_1 = \frac{a_1}{A_{11(1)} s_1} e^{s_1 x} + \frac{a_2}{A_{11(1)} s_2} e^{s_2 x} + \frac{P}{2w} \frac{1}{A_{11(1)} + A_{11(2)}} x + a_3 \quad (\text{A.47})$$

$$U_2 = -\frac{a_1}{A_{11(1)} s_1} e^{s_1 x} - \frac{a_2}{A_{11(1)} s_2} e^{s_2 x} + \frac{P}{2w} \frac{1}{A_{11(1)} + A_{11(2)}} x + a_3 \quad (\text{A.48})$$

$$\beta_1 = \frac{1}{A_{55(1)}} [a_1 k_1 s_1 e^{s_1 x} + a_2 k_2 s_2 e^{s_2 x} + \frac{h_1}{2} (a_1 s_1 e^{s_1 x} + a_2 s_2 e^{s_2 x})] \quad (\text{A.49})$$

$$\beta_2 = \frac{1}{A_{55(2)}} [a_1 k_3 s_1 e^{s_1 x} + a_2 k_4 s_2 e^{s_2 x} + \frac{h_2}{2} (a_1 s_1 e^{s_1 x} + a_2 s_2 e^{s_2 x})] \quad (\text{A.50})$$

The constants a_1 , a_2 and a_3 occurring in the solutions are determined using the boundary conditions. For sublaminate 3 the governing equations are

$$N_{3,x} = 0 \quad (\text{A.51})$$

$$Q_{3,x} + P_3 = 0 \quad (\text{A.52})$$

$$M_{3,x} - Q_3 = 0 \quad (\text{A.53})$$

$$N_3 = A_{11(2)}U_{3,x} \quad (\text{A.54})$$

$$Q_3 = A_{55(2)}\beta_3 \quad (\text{A.55})$$

$$M_3 = D_{11(2)}\beta_{3,x} \quad (\text{A.56})$$

Matching U at the 2-3 interface and applying $N_3(a) = 0$ gives

$$N_3 = 0 \quad (\text{A.57})$$

$$U_3 = U_2(0) \quad (\text{A.58})$$

$$= -\frac{a_1}{s_1 A_{11(2)}} - \frac{a_2}{s_2 A_{11(2)}} + a_3 \quad (\text{A.59})$$

In order to solve for the bending moment, eqs. A.53, A.55 and A.56 are combined to obtain

$$M_{3,xx} - \frac{A_{55(2)}}{D_{11(2)}}M_3 = 0 \quad (\text{A.60})$$

The solution of eq. A.60 can be written as

$$M_3 = \phi_1 \sinh \omega_3 x + \phi_2 \cosh \omega_3 x \quad (\text{A.61})$$

where the quantity ω_3 is defined by

$$\omega_3^2 = \frac{A_{55(2)}}{D_{11(2)}} \quad (\text{A.62})$$

Since the β matching condition cannot be used at the 2-3 interface, the (remaining) boundary conditions are

$$\left. \begin{aligned} M_3(a) &= 0 \\ M_3(0) &= M_2(0) \end{aligned} \right\} \quad (\text{A.63})$$

The ϕ s can be solved using the boundary conditions A.63 as

$$\phi_2 = a_1 k_3 + a_2 k_4 \quad (\text{A.64})$$

$$\phi_1 = -\phi_2 \coth \omega_3 a \quad (\text{A.65})$$

The solution for sublaminates 3 can be completed by writing the following expressions.

$$Q_3 = \phi_1 \omega_3 \cosh \omega_3 x + \phi_2 \omega_3 \sinh \omega_3 x \quad (\text{A.66})$$

$$\beta_3 = \frac{1}{A_{55(2)}} [\phi_1 \omega_3 \cosh \omega_3 x + \phi_2 \omega_3 \sinh \omega_3 x] \quad (\text{A.67})$$

$$P_3 = \frac{A_{55(2)}}{D_{11(2)}} [\phi_1 \sinh \omega_3 x + \phi_2 \cosh \omega_3 x] \quad (\text{A.68})$$

The equilibrium equations for sublaminates 4 are

$$N_{4,x} = 0 \quad (\text{A.69})$$

$$Q_{4,x} = 0 \quad (\text{A.70})$$

$$M_{4,x} - Q_4 = 0 \quad (\text{A.71})$$

The constitutive relations take the form

$$N_4 = A_{11(1)} U_{4,x} \quad (\text{A.72})$$

$$Q_4 = A_{55(1)} (\beta_4 + W_{4,x}) \quad (\text{A.73})$$

$$M_4 = D_{11(1)} \beta_{4,x} \quad (\text{A.74})$$

Using eq. A.69 with the boundary condition $N_4(a) = \frac{P}{2w}$ yields

$$N_4 = \frac{P}{2w} \quad (\text{A.75})$$

Similarly, using eq. A.70 with $Q_4(a) = 0$ results in

$$Q_4 = 0 \quad (\text{A.76})$$

Matching M_1 and M_4 at the 1-4 interface and using eq. A.71 gives

$$M_4 = a_1 k_1 + a_2 k_2 \quad (\text{A.77})$$

The U_4 displacement is obtained by integrating eq. A.72 and using the displacement matching boundary condition $U_4(0) = U_1(0)$.

$$U_4 = \frac{P}{2w} \frac{1}{A_{11(1)}} x + \frac{a_1}{s_1 A_{11(1)}} + \frac{a_2}{s_2 A_{11(1)}} + a_3 \quad (\text{A.78})$$

Similarly, integrating eq. A.74 and setting $\beta_4(a) = 0$ gives

$$\beta_4 = \frac{1}{D_{11(1)}} [a_1 k_1 + a_2 k_2] (x - a) \quad (\text{A.79})$$

Using the solutions for Q_4 and β_4 and the boundary condition $W_4(0) = 0$ in eq. A.73 yields the following solution for W_4 .

$$W_4 = \frac{A_{55(1)}}{D_{11(1)}} [a_1 k_1 + a_2 k_2] \left(\frac{x^2}{2} - ax \right) \quad (\text{A.80})$$

In order to determine a_1 , a_2 and a_3 , the following boundary conditions are used.

$$N_1(0) = \frac{P}{2w}$$

$$\beta_1(0) = \beta_4(0)$$

$$U_1(-l + a) = 0$$

It is convenient to define the following parameters.

$$\theta_1 = \frac{s_1}{A_{55(1)}} \left(k_1 + \frac{h_1}{2} \right) \quad (\text{A.S1})$$

$$\theta_2 = \frac{k_1}{D_{11(1)}} \quad (\text{A.S2})$$

$$\theta_3 = \frac{s_2}{A_{55(1)}} \left(k_2 + \frac{h_1}{2} \right) \quad (\text{A.S3})$$

$$\theta_4 = \frac{k_2}{D_{11(1)}} \quad (\text{A.S4})$$

$$\theta_d = \theta_3 - \theta_1 + (\theta_4 - \theta_2)a \quad (\text{A.S5})$$

The nominal (far field) strain is given by

$$\epsilon = \frac{P}{2w} \frac{1}{A_{11(1)} + A_{11(2)}} \quad (\text{A.S6})$$

The a parameters are obtained as

$$a_1 = A_{11(2)} \epsilon \frac{\theta_3 + \theta_4 a}{\theta_d} \quad (\text{A.87})$$

$$a_2 = -A_{11(2)} \epsilon \frac{\theta_1 + \theta_2 a}{\theta_d} \quad (\text{A.88})$$

$$a_3 = \epsilon(l - a) - \frac{a_1}{s_1 A_{11(1)}} e^{-s_1(l-a)} - \frac{a_2}{s_2 A_{11(1)}} e^{-s_2(l-a)} \quad (\text{A.89})$$

The specimen compliance C is defined as the ratio of specimen extension to applied load. This is obtained as

$$\begin{aligned} C &= \frac{2U_4(a)}{P} \\ &= \frac{2}{P} \left\{ \frac{Pa}{2wA_{11(1)}} + \frac{a_1}{s_1 A_{11(1)}} + \frac{a_2}{s_2 A_{11(1)}} + a_3 \right\} \end{aligned} \quad (\text{A.90})$$

The total energy release rate associated with the crack (delamination) growth under a constant load P is given by

$$G_T = \frac{P^2}{2w} \frac{dC}{da} \quad (\text{A.91})$$

Using the compliance expression from eq. A.90 in eq. A.91 yields the following expression for G_T .

$$G_T = \frac{P^2}{2w^2} \left(\frac{1}{A_{11(1)}} - \frac{1}{A_{11(1)} + A_{11(2)}} + I_1 - I_2 \right) \quad (\text{A.92})$$

where

$$I_1 = \frac{1}{A_{11(1)} + A_{11(2)}} \frac{A_{11(2)} \theta_2 \theta_3 - \theta_1 \theta_4}{A_{11(1)} \theta_d^2} \left(\frac{1 - e^{-s_1(l-a)}}{s_1} - \frac{1 - e^{-s_2(l-a)}}{s_2} \right) \quad (\text{A.93})$$

$$I_2 = \frac{1}{A_{11(1)} + A_{11(2)}} \frac{A_{11(2)} (\theta_3 + \theta_4 a) e^{-s_1(l-a)} - (\theta_1 + \theta_2 a) e^{-s_2(l-a)}}{A_{11(1)} \theta_d} \quad (\text{A.94})$$

The individual fracture mode contributions to the energy release rate can be calculated using the virtual crack closure method, based on the interlaminar stresses and displacements in the vicinity of the crack tip. From the assumed plane strain

condition, the mode III contribution is zero ($G_{III} = 0$). The mode II energy release rate, G_{II} , is calculated using the virtual crack closure technique while G_I is evaluated using

$$G_I = G_T - G_{II} \quad (\text{A.95})$$

G_{II} is calculated from the interlaminar shear stress and relative sliding displacement as

$$G_{II} = \lim_{\delta \rightarrow 0} \frac{1}{2\delta} \int_0^\delta T_1(x - \delta) \Delta u(x) dx \quad (\text{A.96})$$

In the absence of a singularity in the stress field, the result of the limiting process leads to the trivial result $G_{II} = 0$. Hence, the limit is calculated as δ tends to some finite value, say Δ . The value of Δ is chosen depending on the decay length associated with the problem i.e. the length within which the presence of the crack significantly alters the specimen response in comparison with the corresponding far field values. Evidently, the decay length in this problem is dependent on the eigenvalues s_1 and s_2 . The following value of Δ has been chosen in order to reasonably fulfil the decay length criterion.

$$\Delta = \frac{1}{4} \left(\frac{1}{s_1} + \frac{1}{s_2} \right) \quad (\text{A.97})$$

The relative sliding displacement Δu is based only on the difference $U_4 - U_3$ so that the kinematic condition of zero relative displacement at the crack tip is fulfilled. This also simplifies the calculations. The mode II energy release rate component is obtained as

$$G_{II} = \frac{I_3 + I_4}{2\Delta} \quad (\text{A.98})$$

where I_3 and I_4 are defined as

$$I_3 = \left(\frac{1}{A_{11(1)}} + \frac{1}{A_{11(2)}} \right) \left(\frac{a_1}{s_1} + \frac{a_2}{s_2} \right) \left[a_1(1 - e^{-s_1\Delta}) + a_2(1 - e^{-s_2\Delta}) \right] \quad (\text{A.99})$$

$$I_4 = \left(\frac{s_1 \Delta - 1 + e^{-s_1 \Delta}}{s_1} a_1 + \frac{s_2 \Delta - 1 + e^{-s_2 \Delta}}{s_2} a_2 \right) \epsilon \frac{A_{11(1)} + A_{11(2)}}{A_{11(1)}} \quad (\text{A.100})$$

Transverse Crack Spacing

Shear Deformation Model

The model presented so far has dealt with delaminations growing from a transverse crack. The same model can be modified to predict the spacing of these transverse cracks. In order to accomplish this, the delamination effect has to be isolated from the model. This can be achieved approximately by letting the crack length a tend to zero. This yields an approximation since the boundary conditions are not accounted for properly by this limiting process. To get an accurate shear deformation model, we consider only sublaminates 1 and 2 and apply the following boundary conditions for sublaminate 2:

$$N_2(0) = 0 \quad (\text{A.101})$$

$$M_2(0) = 0 \quad (\text{A.102})$$

Using these boundary conditions in eqs. A.37 and A.44 yields two equations in a_1 and a_2 which can be solved to obtain

$$a_1 = \frac{k_4}{k_4 - k_3} \frac{P}{2w} \frac{A_{11(2)}}{A_{11(1)} + A_{11(2)}} \quad (\text{A.103})$$

$$a_2 = \frac{k_3}{k_3 - k_4} \frac{P}{2w} \frac{A_{11(2)}}{A_{11(1)} + A_{11(2)}} \quad (\text{A.104})$$

The interlaminar shear stress can now be obtained using eq. A.45. The saturation crack spacing corresponds to the distance from the crack where the broken plies regain their uniform stress/strain state i.e. where the interlaminar shear stress has decayed down to its far field (uniform) value. Practically, this distance is calculated by looking for the x where the interlaminar shear stress is some small fraction (say

.001) of its maximum value. The maximum shear stress evidently occurs at $x = 0$ and is given by

$$T_1^{(max)} = a_1 s_1 + a_2 s_2 \quad (\text{A.105})$$

The crack spacing λ can then be determined by solving the following transcendental equation.

$$\frac{a_1 s_1 e^{s_1 \lambda} + a_2 s_2 e^{s_2 \lambda}}{a_1 s_1 + a_2 s_2} = 0.001 \quad (\text{A.106})$$

Membrane Model

A simpler model can be used to estimate the saturation spacing of the transverse cracks. This model treats the sublaminates as membranes i.e. the bending effects are ignored. The equilibrium equations for a generic membrane sublaminate are

$$N_{,x} + T_t - T_b = 0 \quad (\text{A.107})$$

$$\frac{h}{2}(T_t - T_b) - Q = 0 \quad (\text{A.108})$$

The constitutive equations take the form

$$N = \left(A_{11} - \frac{B_{11}^2}{D_{11}} \right) U_{,x} \quad (\text{A.109})$$

$$Q = A_{55} \beta \quad (\text{A.110})$$

The displacements are assumed to be of the following form.

$$u = U(x) + z\beta(x) \quad (\text{A.111})$$

$$w = 0 \quad (\text{A.112})$$

The following governing equations can now be written

$$N_{1,x} - T_1 = 0 \quad (\text{A.113})$$

$$N_{2,x} + T_1 = 0 \quad (\text{A.114})$$

$$\frac{h_1}{2}T_1 - Q_1 = 0 \quad (\text{A.115})$$

$$\frac{h_2}{2}T_1 - Q_2 = 0 \quad (\text{A.116})$$

$$N_1 = \gamma_1 U_{1,x} \quad (\text{A.117})$$

$$N_2 = \gamma_2 U_{2,x} \quad (\text{A.118})$$

$$Q_1 = A_{55(1)}\beta_1 \quad (\text{A.119})$$

$$Q_2 = A_{55(2)}\beta_2 \quad (\text{A.120})$$

$$U_1 - \frac{h_1}{2}\beta_1 = U_2 + \frac{h_2}{2}\beta_2 \quad (\text{A.121})$$

where the γ s are defined as

$$\gamma_1 = A_{11(1)} - \frac{B_{11(1)}^2}{D_{11(1)}} \quad (\text{A.122})$$

$$\gamma_2 = A_{11(2)} - \frac{B_{11(2)}^2}{D_{11(2)}} \quad (\text{A.123})$$

Eqs. A.113 and A.115 can be combined as

$$Q_1 = \frac{h_1}{2}N_{1,x} \quad (\text{A.124})$$

Using eqs. A.119 and A.117 in this leads to

$$\beta_1 = \frac{h_1}{2} \frac{1}{A_{55(1)}} \gamma_1 U_{1,xx} \quad (\text{A.125})$$

Following a similar procedure for β_2 yields

$$\beta_2 = \frac{h_2}{2} \frac{1}{A_{55(2)}} \gamma_1 U_{1,xx} \quad (\text{A.126})$$

Using these two relations in eq. A.121 leads to

$$U_1 - \left(\frac{h_1}{2}\right)^2 \frac{\gamma_1}{A_{55(1)}} U_{1,xx} = U_2 - \left(\frac{h_2}{2}\right)^2 \frac{\gamma_1}{A_{55(2)}} U_{1,xx} \quad (\text{A.127})$$

Combining eqs. A.113, A.114, A.117 and A.118 gives

$$\gamma_1 U_{1,xx} + \gamma_2 U_{2,xx} = 0 \quad (\text{A.128})$$

Substituting this into eq. A.127 results in

$$U_{1,xx} - \left[\left(\frac{h_1}{2} \right)^2 \frac{\gamma_1}{A_{55(1)}} + \left(\frac{h_2}{2} \right)^2 \frac{\gamma_1}{A_{55(2)}} \right] U_{1,xxxx} + \frac{\gamma_1}{\gamma_2} U_{1,xx} = 0 \quad (\text{A.129})$$

The characteristic roots of this differential equation are

$$s = 0, 0, \pm \sqrt{\frac{\gamma_1 + \gamma_2}{\gamma_1 \gamma_2 \left[\left(\frac{h_1}{2} \right)^2 \frac{1}{A_{55(1)}} + \left(\frac{h_2}{2} \right)^2 \frac{1}{A_{55(2)}} \right]}} \quad (\text{A.130})$$

The solution for U_1 can then be written as

$$U_1 = A_1 e^{s_1 x} + A_2 x + A_3 \quad (\text{A.131})$$

where the A s are arbitrary constants to be determined from the boundary conditions. The root s_1 is the positive root such that a decaying solution is obtained in the negative x region. For the special case of $B_{11(1)} = B_{11(2)} = 0$, the nonzero roots can be written in a simpler form as

$$s^2 = \frac{4(A_{11(1)} + A_{11(2)})}{A_{11(1)} A_{11(2)}} \frac{1}{\frac{h_1^2}{A_{55(1)}} + \frac{h_2^2}{A_{55(2)}}} \quad (\text{A.132})$$

The interlaminar shear stress can be obtained as follows.

$$\begin{aligned} T_1 &= N_{1,x} \\ &= \gamma_1 U_{1,xx} \\ &= \gamma_1 A_1 s_1^2 e^{s_1 x} \end{aligned} \quad (\text{A.133})$$

The maximum shear stress is

$$T_1^{(max)} = \gamma_1 A_1 s_1^2 \quad (\text{A.134})$$

Then, the saturation crack spacing λ corresponds to

$$e^{s_1 \lambda} = 0.001 \quad (\text{A.135})$$

Shear Lag Model

This model allows for a nonlinear displacement field through the thickness of the sublaminate. Its fundamental assumption is that the shear deformation neglected in the classical theory of bending can be estimated using the shear stress. The sublaminate axial force equilibrium condition can be written as

$$N_{,x} + (T_t - T_b) = 0 \quad (\text{A.136})$$

The axial stress is assumed to be uniform and is given by

$$\sigma_{xx} = \frac{N}{h} \quad (\text{A.137})$$

The shear stress is estimated as follows

$$\begin{aligned} \sigma_{xz,z} &= -\sigma_{xx,x} \\ &= \frac{-N_{,x}}{h} \\ &= \frac{T_t - T_b}{h} \end{aligned} \quad (\text{A.138})$$

This can be integrated to obtain

$$\sigma_{xz} = \frac{T_t - T_b}{h} z + \frac{T_t + T_b}{2} \quad (\text{A.139})$$

Neglecting transverse displacement, the axial displacement can be obtained by integrating the shear strain, which in turn is obtained from the shear stress.

$$\begin{aligned} u_{,z} &= \frac{\sigma_{xz}}{C_{55}} \\ &= \frac{1}{C_{55}} \left[(T_t - T_b) \frac{z}{h} + \frac{T_t + T_b}{2} \right] \end{aligned} \quad (\text{A.140})$$

$$u = U(x) + \frac{1}{2C_{55}} \left[(T_t - T_b) \frac{z^2}{h} + (T_t + T_b)z \right] \quad (\text{A.141})$$

where $U(x)$ is the mid-plane axial displacement. This displacement expression can be used to obtain an improved axial stress estimate as follows.

$$\sigma_{xx} = C_{11} u_{,x}$$

$$= C_{11} \left[U_{,x} + \frac{1}{2C_{55}} (T_t - T_b)_{,x} \frac{z^2}{h} + (T_t + T_b)_{,x} z \right] \quad (\text{A.142})$$

The corresponding axial stress resultant can be written as

$$\begin{aligned} N &= \int_{-\frac{h}{2}}^{\frac{h}{2}} \sigma_{zz} dz \\ &= C_{11} \left[h U_{,x} + \frac{h^2}{24C_{55}} (T_t - T_b)_{,x} \right] \end{aligned} \quad (\text{A.143})$$

The governing equations for the sublaminates are thus eqs. A.136 (equilibrium), A.141 (displacement field) and A.143 (constitutive relationship). Using these to model sublaminates 1 and 2 results in the following governing equations.

$$N_{1,x} - T_1 = 0 \quad (\text{A.144})$$

$$N_{2,x} + T_2 = 0 \quad (\text{A.145})$$

$$N_1 = C_{11(1)} \left[h_1 U_{1,x} - \frac{h_1^2}{24C_{55(1)}} T_{1,x} \right] \quad (\text{A.146})$$

$$N_2 = C_{11(2)} \left[h_2 U_{2,x} + \frac{h_2^2}{24C_{55(2)}} T_{1,x} \right] \quad (\text{A.147})$$

$$u_1 = U_1 + \frac{1}{2C_{55(1)}} \left[-T_1 \frac{z^2}{h_1} + T_1 z \right] \quad (\text{A.148})$$

$$u_2 = U_2 + \frac{1}{2C_{55(2)}} \left[T_1 \frac{z^2}{h_2} + T_1 z \right] \quad (\text{A.149})$$

Displacement continuity at the 1-2 interface implies

$$u_1(x, -\frac{h_1}{2}) = u_2(x, \frac{h_2}{2}) \quad (\text{A.150})$$

$$\text{or} \quad U_2 = U_1 - \frac{3T_1}{8} \left[\frac{h_1}{C_{55(1)}} + \frac{h_2}{C_{55(2)}} \right] \quad (\text{A.151})$$

Equation A.146 can be rewritten as

$$U_{1,x} = \frac{N_1}{C_{11(1)} h_1} + \frac{h_1}{24C_{55(1)}} T_{1,x} \quad (\text{A.152})$$

Combining eqs. A.147, A.151 and A.152 results in

$$N_2 = C_{11(2)} \left\{ \frac{h_2 N_1}{h_1 C_{11(1)}} - \frac{h_2 T_{1,x}}{3} \left[\frac{h_1}{C_{55(1)}} + \frac{h_2}{C_{55(2)}} \right] \right\} \quad (\text{A.153})$$

But from eqs. A.144 and A.145, we have

$$N_{2,x} = -T_1 = -N_{1,x} \quad (\text{A.154})$$

Using this in the differentiated form of eq. A.153 leads to

$$\left[\frac{1}{h_2 C_{11(2)}} + \frac{1}{h_1 C_{11(1)}} \right] N_{1,x} = \frac{1}{3} \left[\frac{h_1}{C_{55(1)}} + \frac{h_2}{C_{55(2)}} \right] N_{1,xxx} \quad (\text{A.155})$$

The nonzero characteristic roots of this equation are given by

$$s^2 = 3 \left(\frac{C_{55(1)}}{h_1 C_{11(1)}} \right) \left(\frac{C_{55(2)}}{h_2 C_{11(2)}} \right) \left(\frac{h_1 C_{11(1)} + h_2 C_{11(2)}}{h_2 C_{55(1)} + h_1 C_{55(2)}} \right) \quad (\text{A.156})$$

This is the same as in the membrane model except for the factor 3 which is 4 in the membrane model. This difference is related to the fact that the axial displacement distribution through the thickness is parabolic in the shear lag model and linear in the membrane model. The crack spacing λ for the shear lag model is determined as in the case of the membrane model but using the modified characteristic root.

Table 1 Summary of Results

number of 90° plies	G_T J/m ²	G_{II}/G_T	σ_c MPa	ϵ_c %
1/2	2.404	0.276	1313.9	1.6747
1	6.752	0.275	784.0	1.1685
2	22.849	0.267	426.2	0.8058
3	51.049	0.261	285.1	0.6427
4	93.603	0.256	210.6	0.5444
6	228.871	0.250	134.7	0.4264
8	440.065	0.247	97.1	0.3555

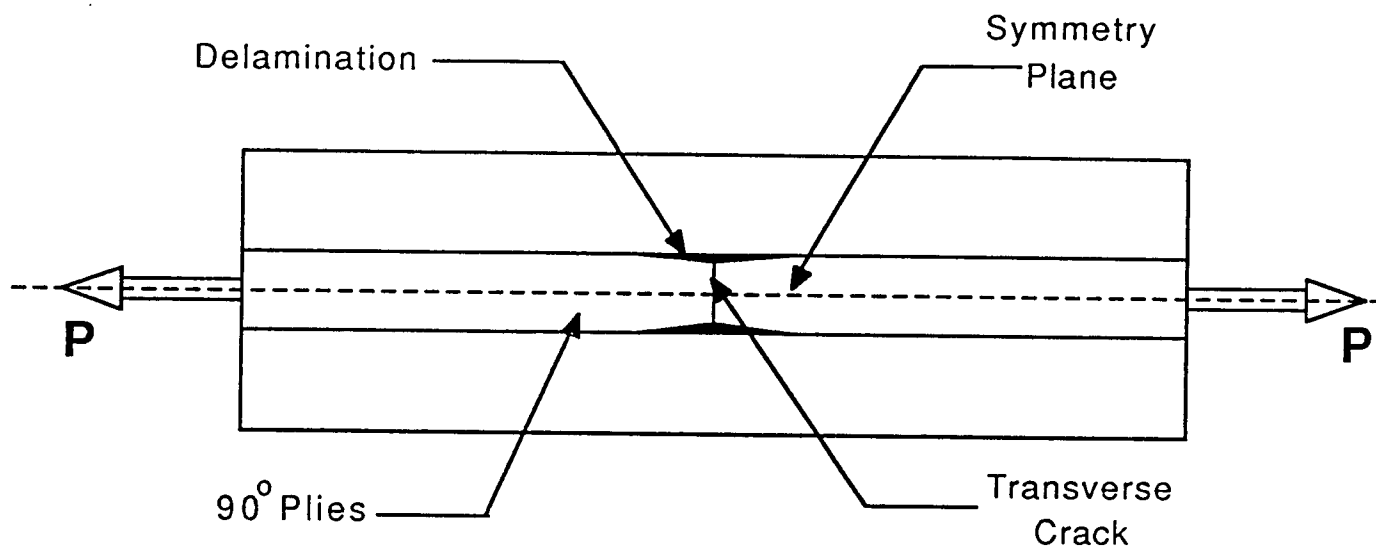


Fig. 1 Specimen Cross Section

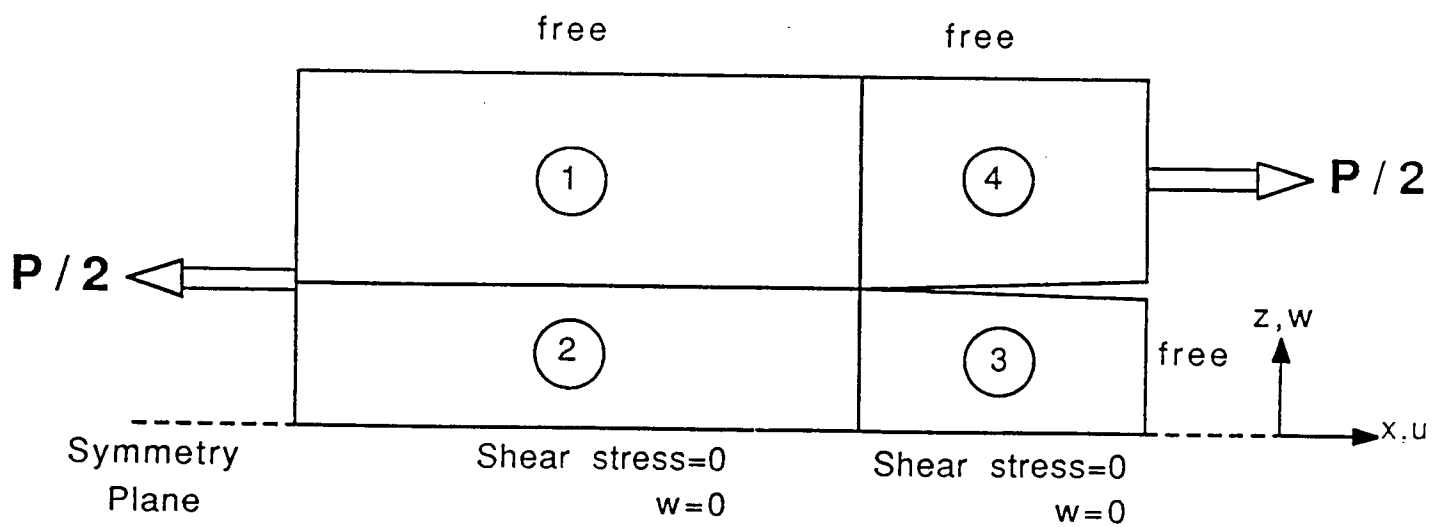


Fig. 2 Modelled Region and Sublamine Scheme

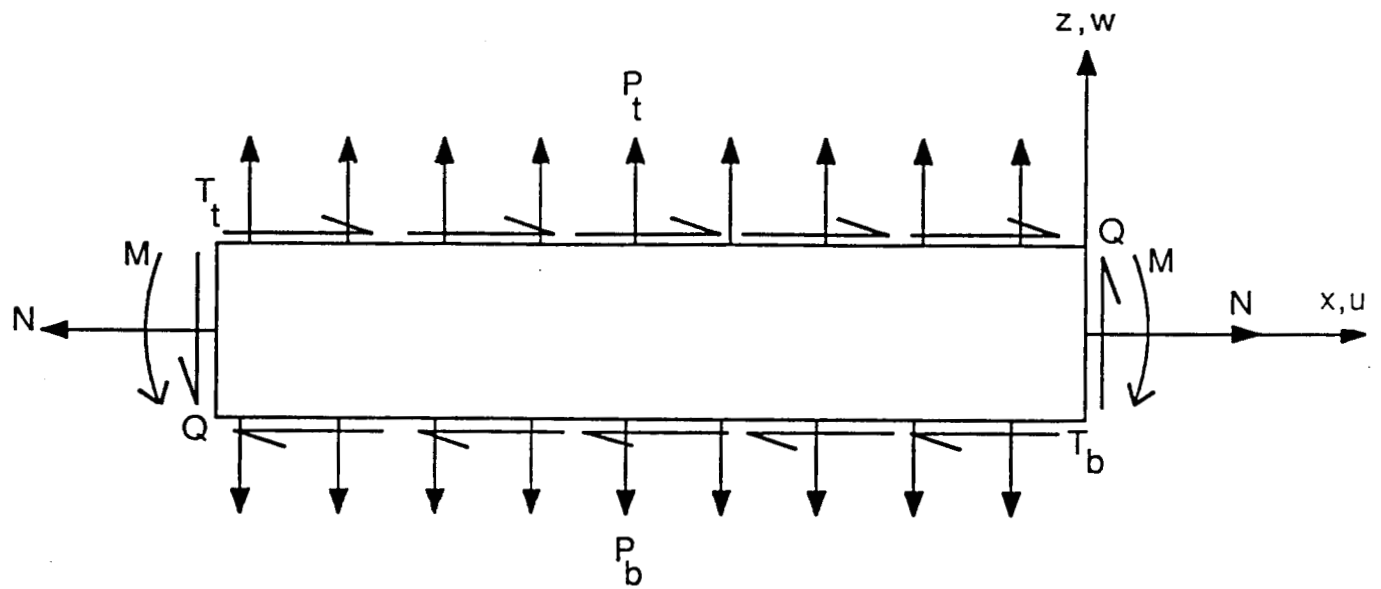


Fig. 3 Generic Sublamine

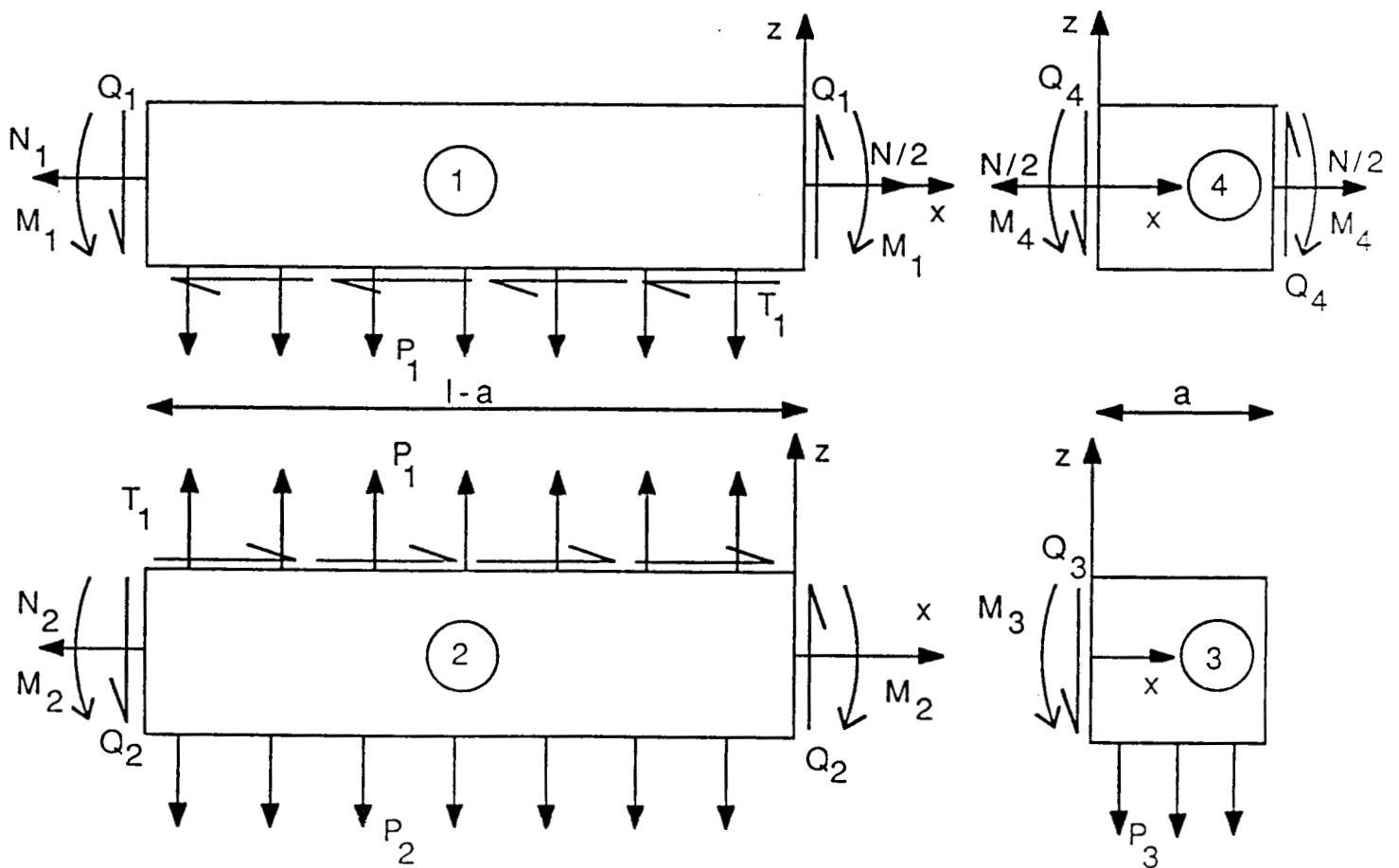


Fig. 4 Sublamine Forces and Coordinate Systems

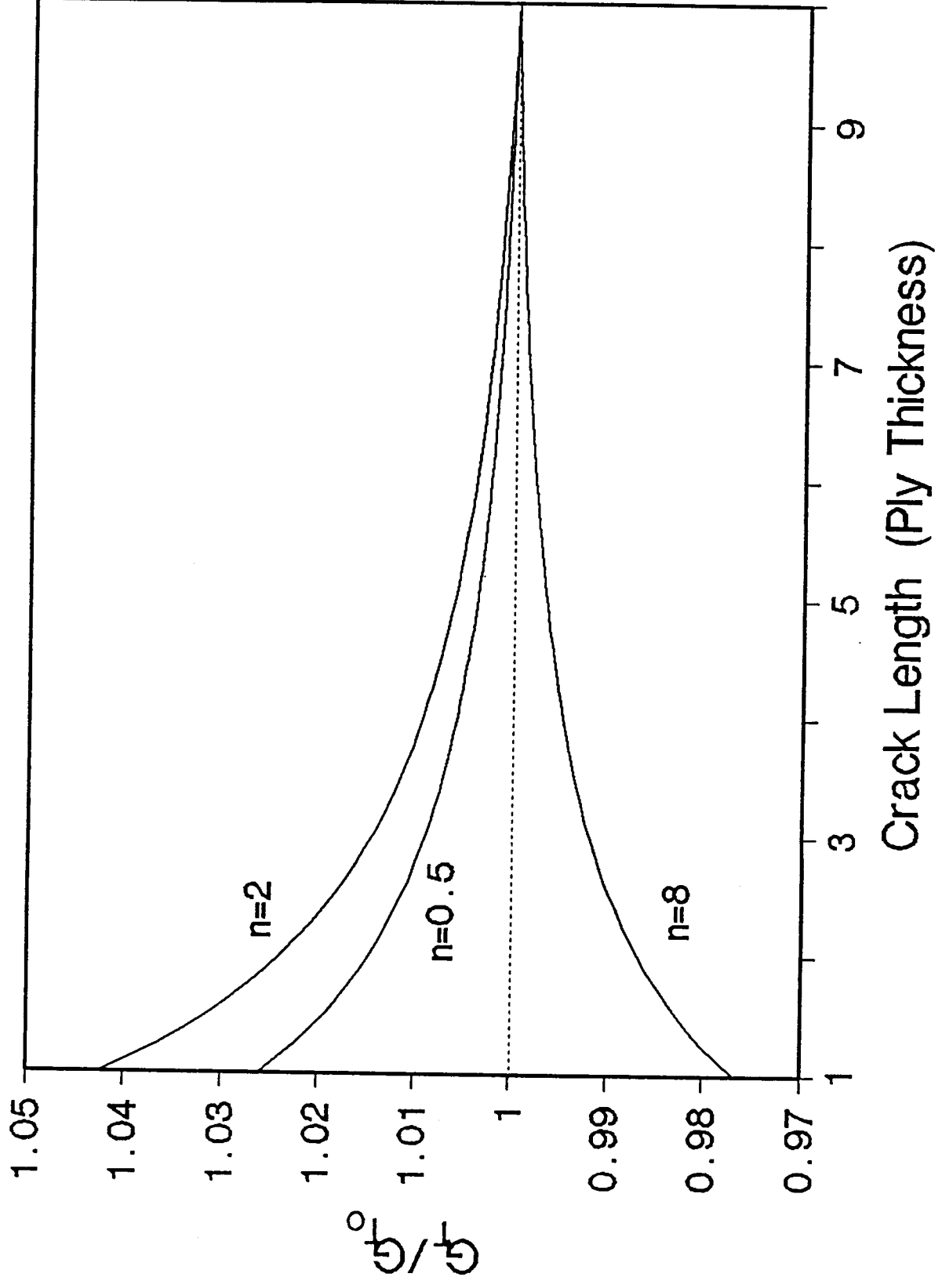


Fig. 5 Total Energy Release Rate Variation with Initial Crack Size

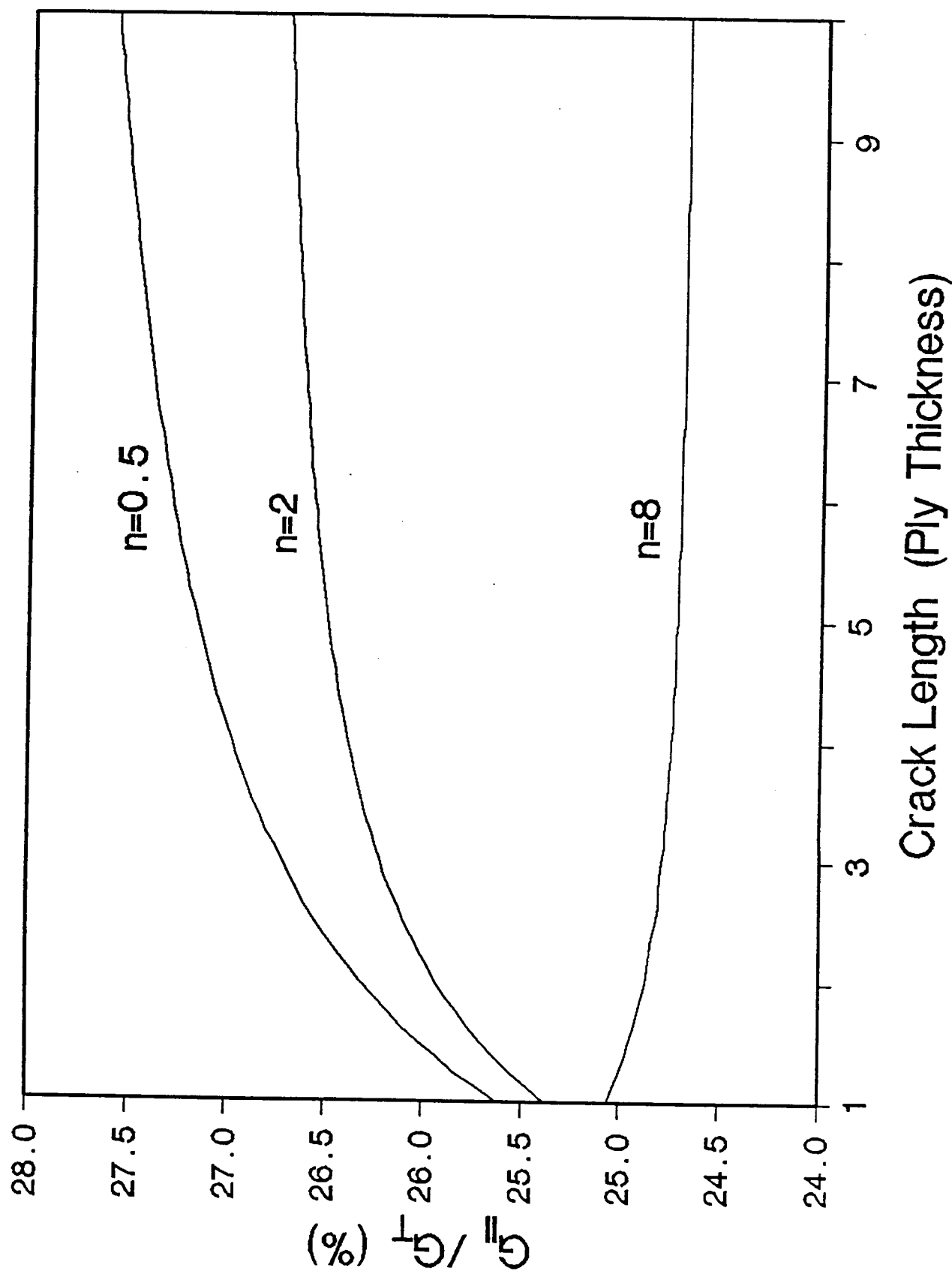


Fig. 6 Mode II Energy Release Rate Dependence on Crack Size

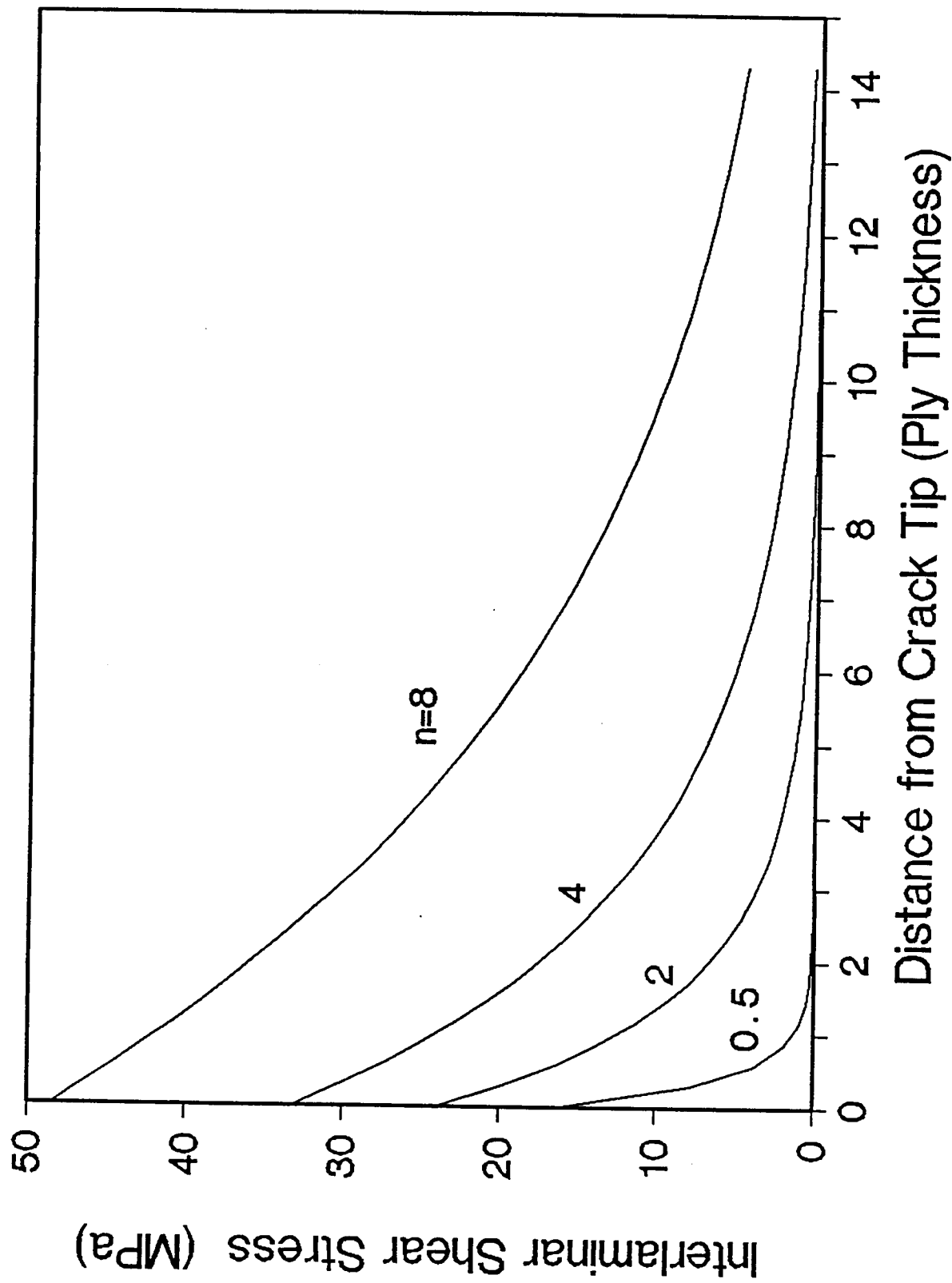


Fig. 7 Interlaminar Shear Stress Distribution

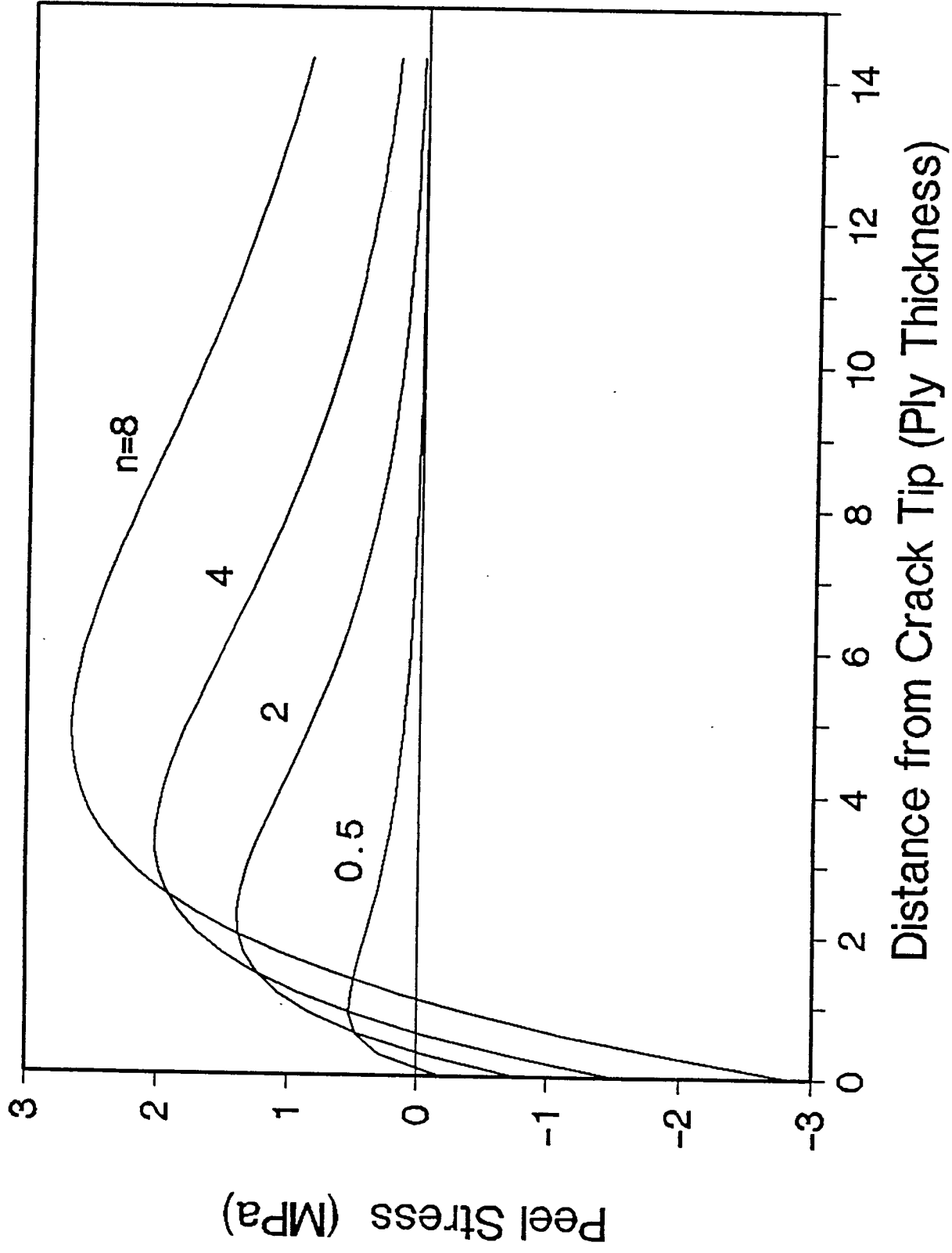
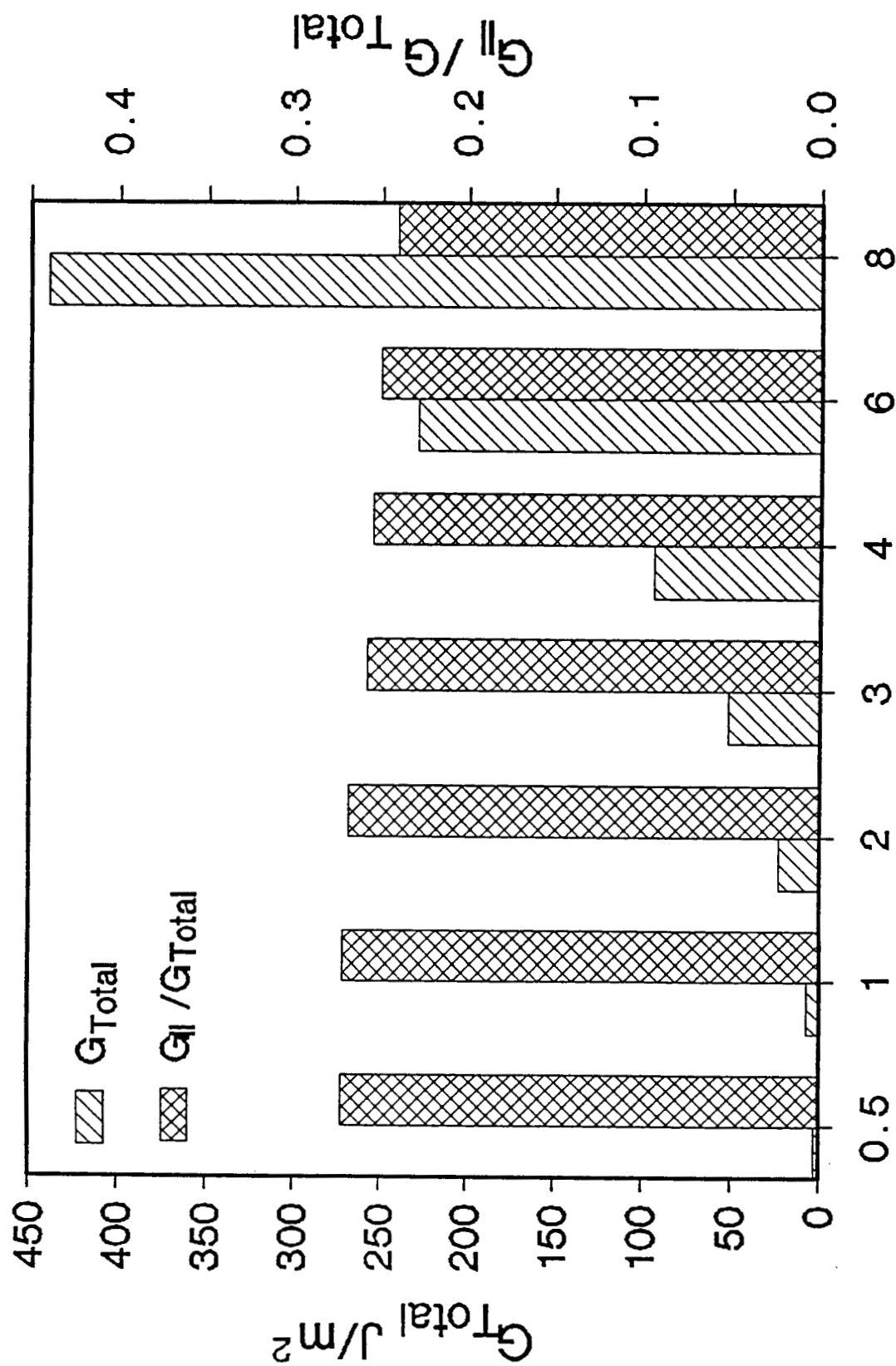


Fig. 8 Interlaminar Normal Stress (Peel Stress) Distribution



Number of 90° plies

Fig. 9 Energy Release Rate Comparison

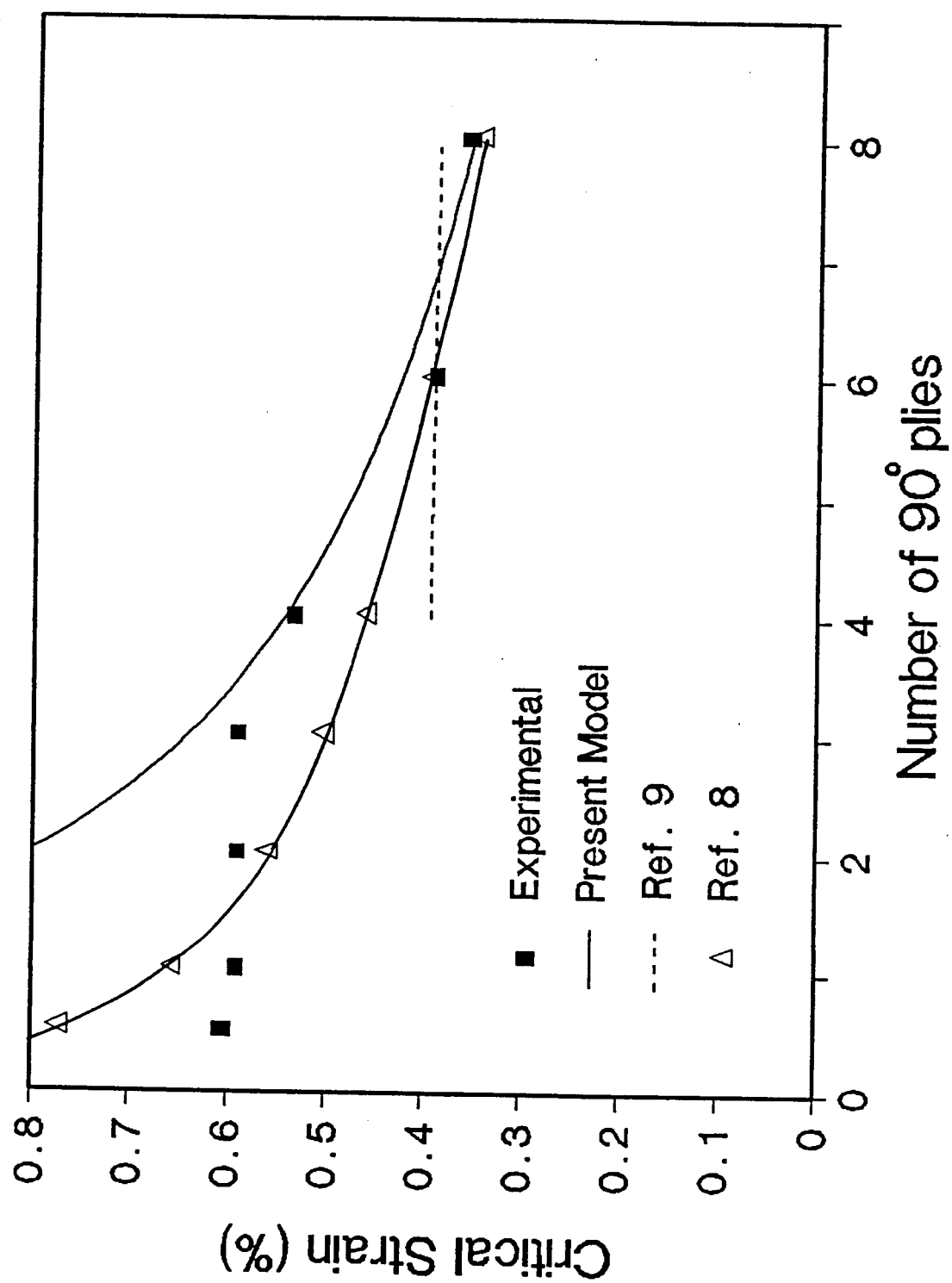


Fig. 10 Critical Delamination Growth Strain Variation